

1 **Sensitivity analysis of input ground motion on surface motion
2 parameters in high seismic regions: A case of Bhutan
3 Himalaya**

4 Karma Tempa¹, Komal Raj Aryal², Nimesh Chettri¹, Giovanni Forte³, Dipendra Gautam^{4,5,6 *}

5 ¹Civil Engineering Department, College of Science and Technology, Royal University of Bhutan,
6 Phuentsholing, Bhutan

7 ²Faculty of Resilience, Rabdan Academy, Abu Dhabi, United Arab Emirates

8 ³Department of Civil, Environmental and Architectural Engineering (DICEA), University of Naples Federico II,
9 Naples, Italy

10 ⁴Department of Civil Engineering, Institute of Engineering, Thapathali Campus, Kathmandu, Cosmos College of
11 Management and technology, Lalitpur, Nepal

12 ⁵Department of Civil Engineering, Institute of Engineering, Thapathali Campus, Kathmandu, Nepal

13 ⁶Interdisciplinary Research Institute for Sustainability, Kathmandu, Nepal

14 * Correspondance: Dipendra Gautam (dipendra01@tcioe.edu.np)

15 **Abstract.** Historical earthquakes ~~have demonstrated~~^{depicted} that strong motion characteristics and local soil
16 condition, when coupled, significantly influence seismic site response. ~~Interestingly, m~~ost of the Himalayan
17 earthquakes ~~have~~ depicted anomalous behavior per the site conditions historically. Being one of the most active
18 seismic regions on earth, the eastern fringe of the Himalaya has observed many devastating earthquakes ~~together~~
19 ~~with non-uniform damage scenarios, and uneven damages were extensively reported.~~ To ~~quantify such~~
20 ~~anomalies, this end~~, we ~~present evaluate~~^{quantification of} surface motion parameters for a soft soil deposit
21 located at Phuentsholing ~~C~~ity in western Bhutan. Using one dimensional site response analysis, sensitivity of
22 ground motion variation is estimated ~~for Bhutan~~. This study accounts for the earthquakes of moment
23 magnitude~~s between 6.6 and to~~ 7.5 with a wide variation of peak ground acceleration (PGA)~~even beyond~~
24 0.28g, ~~which is the maximum PGA range suggested by the Global Seismic Hazard Map (GSHAP).~~ To dissect
25 the characteristics of six inputted ground motions on eight local ground conditions, sensitivity analysis is
26 performed statistically. The statistical correlation of the response data sets and the linear regression model of the
27 bedrock outcrop and the surface motion spectral acceleration along the stratified depth ~~were are~~ examined to
28 quantify the variation in surface motion parameters. The ~~r~~esults highlighted that the strong motions ~~having~~
29 ~~with~~ PGA greater than 0.34-g demonstrate greater sensitivity, leading to some anomalies in response parameters,
30 ~~especially amplification. Similar results were obtained for the low PGA range (<0.1g), resulting in attenuation~~
31 ~~of seismic site effect (amplification). The same scenario was observed for the PGA range below 0.1g.~~

32 **Keywords:** seismic site effect, amplification factor, soil fundamental period, sensitivity analysis, Bhutan.

33 **1. Introduction**

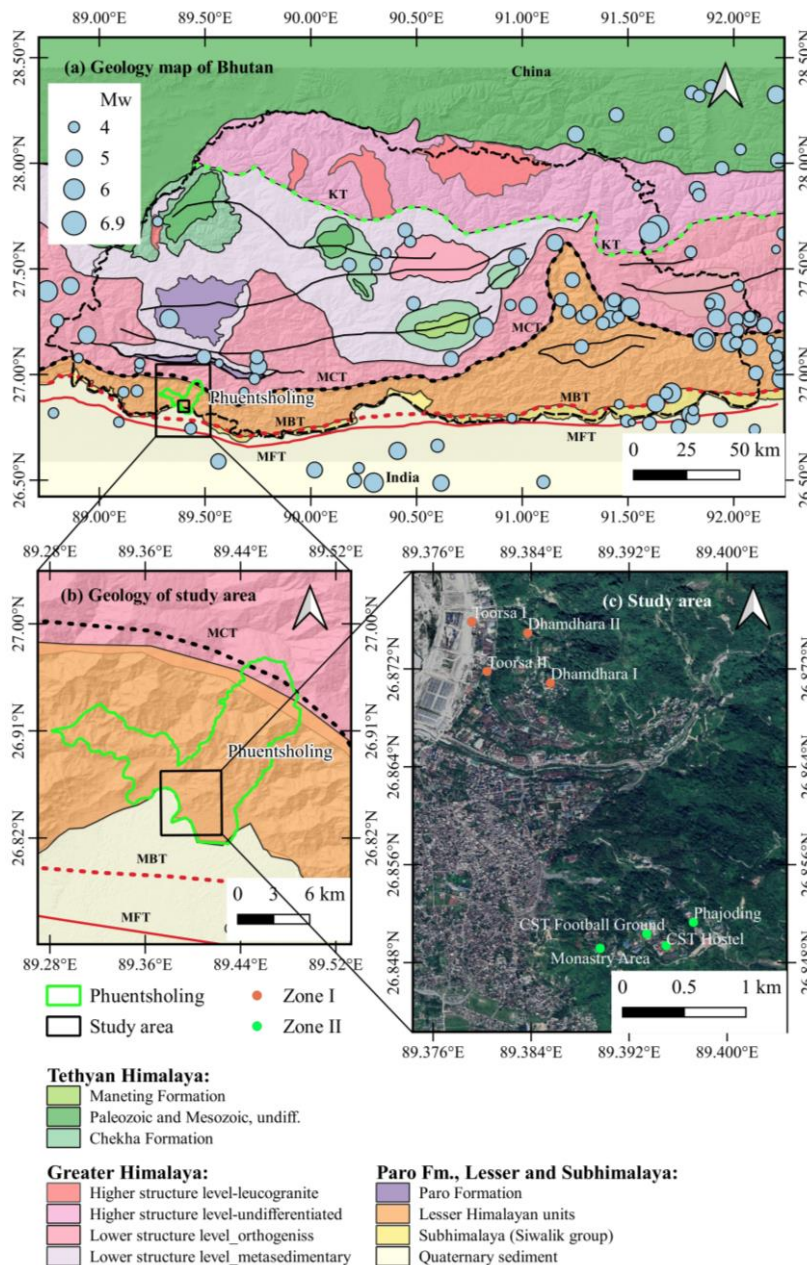
34 Bhutan is located in the eastern fringe of Hindu-Kush-Himalaya. Historical earthquakes that occurred in the
35 Hindu-Kush-Himalayan region have resulted in enormous losses and damages (Gautam et al., 2016). Akin to

36 ~~the historical earthquakes, and thus~~ the impending earthquakes are certain to strike the region ~~with and result in~~
37 detrimental consequences. The eastern fringe of Himalaya, i.e., Bhutan, and neighboring areas were strongly
38 ~~affected shaken~~ by significant earthquakes in the past; however, most of the ~~e earthquakes~~ ~~that~~ occurred until
39 the 18th century are not well ~~documented~~. The most recent events ~~occurred on such as the~~ April 05, 2021 (M_w
40 5.0) in Samtse (South Bhutan) and ~~the in~~ September 2009 Mongar earthquake (M_w 6.7) in eastern Bhutan
41 ~~manifested widespread damage to Bhutan and neighboring regions~~. These earthquakes caused major damages in
42 the eastern parts of Bhutan and considerably affected ~~the other parts of the Country~~ ~~the other parts of the country~~
43 (Chettri et al., 2021b). All the past earthquakes highlighted anomalous damage pattern to structures and
44 infrastructures in various parts of the country, especially in the plain areas. ~~Such This~~ evidence ~~prompt~~
45 ~~indication of~~ ~~indicates the~~ likely local site effects in Bhutan. So far, few studies on local seismic response ~~have~~
46 ~~been conducted are~~ in Bhutan, using a single strong motion ~~record~~, but the ~~reported~~ studies mainly focused on
47 the role of bedrock depth ~~on in~~ ground response parameters (Tempa et al., 2020) (Tempa et al., 2021). The
48 ground motion response analysis may not adequately address the accuracy in predicting the response ~~parameters~~
49 ~~due to when the information is limited~~ ~~information~~ regarding site characteristics and their variations within the
50 same soil column (Stevens et al., 2020). In the case of data scarce regions such as Bhutan, the variation in
51 terms of material characteristics can be possibly accounted for using sensitivity analysis. For this reason, this
52 study quantifies the characteristics and effects of several strong ground motions ~~to site effects depiction~~. Seismic
53 ground response analysis fall in the Grade III approach of microzonation studies (e.g. ISSMGE 1999; Licata et
54 al., 2018). It is widely used method ~~widely~~ by researchers for various applications in order to capture local
55 ground effects or site conditions that can affect the estimate ~~and prediction~~ of ground motion characteristics
56 (Chavez-Garcia et al., 1990); (Lopez-Caballero et al., 2012) (Gautam & Chamlagain, 2016), (Sil & Haloi,
57 2018)). The outcomes of such studies aim to provide local seismic hazard parameters, which can be adopted for
58 design of structures and infrastructures (Douglas, 2006). Ground response parameters typically characterize the
59 complex nature of strong motion accelerograms using a simple expansion of predictive relationships. The
60 ~~two~~ ~~Two~~ prominent ~~approaches~~, deterministic and probabilistic, ~~approaches~~ are widely used for seismic hazard
61 studies ~~globally~~. Previously, (Tempa et al., 2021) recommended the use of the deterministic approach that can
62 estimate ~~the~~ parameters under various earthquake occurrence scenarios. Notably, selecting a single ground
63 motion considering amplitude ~~only~~ for seismic ~~hazard site response~~ analysis may not be a reliable approach to
64 estimate site amplification. ~~The selection~~ Selection of a wide amplitude range and the assessment of likely
65 fluctuation scenario for Bhutan is not done yet. Hence, ground motion parameters that are related to the
66 amplitude are investigated to examine and predict the variability, often regarded as sensitivity, concerning mean
67 values and associated scatter.

68 In this paper, sensitivity analysis of site response for specific soil conditions in Phuentsholing, Bhutan is
69 explored by a statistical correlation function of the ground motion parameters for different earthquake shaking
70 intensities. The study area is one of the major urban and commercial hubs in Bhutan Himalaya and seismic site
71 effects on existing structures may have detrimental consequences due to inherent vulnerabilities of structures
72 and infrastructures as well as due to the likely phenomenon such as amplification ~~effects~~ in loose soil deposits.
73 To quantify the seismic site effects in terms of amplification of amplitude parameters, a range of time histories
74 is selected, and site response parameters are estimated.

75 2. Seismicity and geology of the study area

76 The Himalayan regionHimalaya is one of the most seismically active regions on earth, which observes both
77 large and moderate-sized events frequently (Drukpa et al., 2006). Bhutan is located in the eastern Himalayas
78 formed due to the subduction of the Indian Pplate beneath the Eurasian PPlate and spans from the low-lying
79 Brahmaputra Plain to the high Tibetan Plateau. Most of the land area of Bhutan is underlain by the Main
80 Himalayan Thrust (MHT), which runs along the entire length of the Himalayan arc. Historical earthquake
81 catalog (see Fig. 1a) indicates that Bhutan has experienced several earthquakes of moment magnitude greater
82 than 5.0 since early 1900, among them, the 1915 Trashigang (M_w 6.6), 1954 TrashiYangtse (M_w 6.4), and in the
83 2009 Mongar (M_w 6.1) earthquakes that occurred at 11 km east of Bhutan are the most notable ones. The 2011
84 Sikkim-Nepal earthquake (M_w 6.9) also caused noticeable damage to building stocks in Bhutan (Chettri et al.,
85 2021a). The earthquakes in the vicinity of the study area (Phuentsholing) include the 1981 Dagana (M_w 5.1)
86 earthquake and the 2003 Haa earthquake (M_w 5.5). The most recent event occurred in Samtse in 2021 (M_w 5.1)
87 affected Phuentsholing and the neighboring areas with an intensity level of IV in Modified Mercalli Intensity
88 (MMI) scale (Gautam et al., 2022). Continuity of seismic activities in Bhutan is attributed to the presence of
89 major shear zones such as the Main Himalaya Thrust (MHT), Main Boundary Thrust (MBT), Main Central
90 Thrust (MCT), and the South Tibetan Detachment System (STDS) (Long & McQuarrie, 2010) as shown in
91 Figure 1a. The study area is within the Phuentsholing FFormation of Buxa group of the Lesser Himalaya, mainly
92 characterized by highly weathered dark grey to black slate and phyllite, thin interbedding of limestone with
93 substantial amount of cream-colored dolomite and fine-medium quartzite, additionally consisting fine to
94 medium grained conglomeratic quartzite interbedded with phyllite and dolomite towards the Rinchending area
95 of Zone II. Hence, the lithological characteristic of the area indicates weak and highly unstable geology in the
96 region. The presence of thrust faults in the proximity of the study area along the entire belt of the Lesser
97 Himalayan units and the quaternary sediments in the south depict the area to be seismically active with the
98 majority of the historical earthquake events concentrated within these geological units. In particular, this study
99 focuses on Phuentsholing Thromde (city)city of Chhukha dzongkhag (district)district in Bhutan (Fig. 1c). The
100 city is one of the major commercial hubs for trade with India. The proposed study area is observing rapid
101 infrastructure development activities and urban expansion for residential, commercial, and industrial purposes.
102 The Phuentsholing city covers an area of 15.6 km² and is located at 26.86°E and 89.39°N. The city has the
103 population of 27,658 people, mostly distributed towards the peripheral international border area with a total of
104 2,263 residential and commercial buildings per the 2020 statistics (<http://www.pcc.bt/index.php/>). The seismic
105 site characterization includes eight locations in the regions of Dhamdhara, Toorsa, and Rinchending in
106 Phuentsholing, Bhutan. In this study, the sites are grouped into two main zones based on the geographical
107 location and immediate availability of survey locations. These two zones also refer to the Local Area Plan
108 (LAP) of Phuentsholing. The zones are Zone I: Dhamdhara I, Dhamdhara II, Toorsa I, and Toorsa II, and Zone
109 II: College of Science and Technology (CST) Football Ground, CST Hostel, Phajoding, and the Monastery area.
110 Among the 8 LAPs, Dhamdhara and Toorsa (Zone I) are in the same region in the western part of the city and
111 Rinchending (Zone II) is in the east.
112



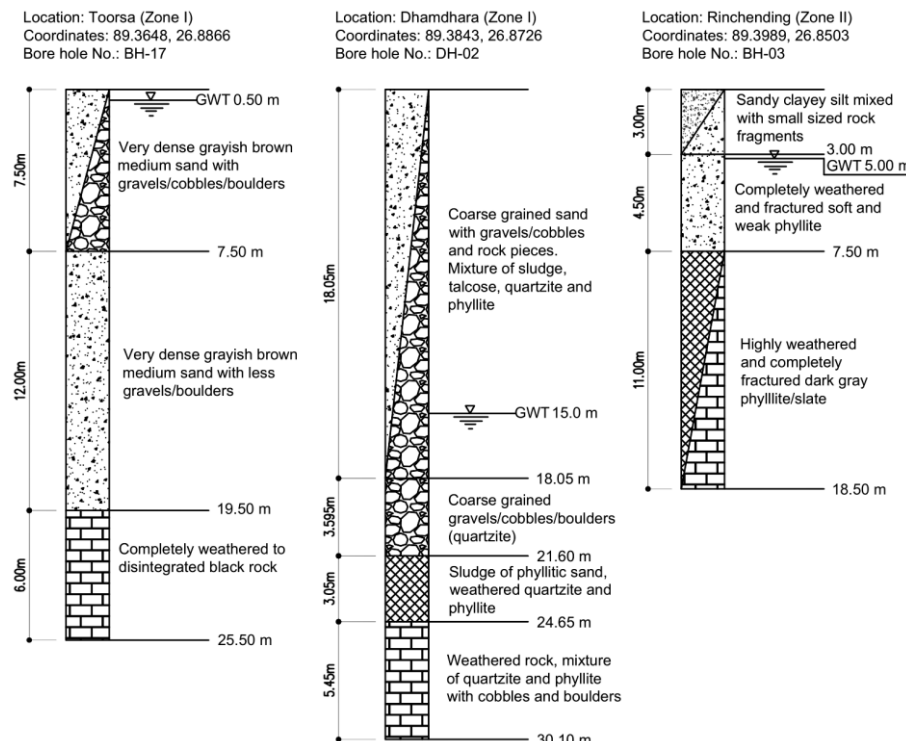
113

114 **Figure 1:** Geology and seismicity and the study area: (a) Geological map of Bhutan reproduced from
 115 (McQuarrie et al., 2013) and seismicity, (b) Location of Phuentsholing and geology of the area, (c) Study area
 116 showing surveyed site using MASW (modified from Google Earth Pro 2021).

117 3. Materials and method

118 3.1 Geotechnical site characterization

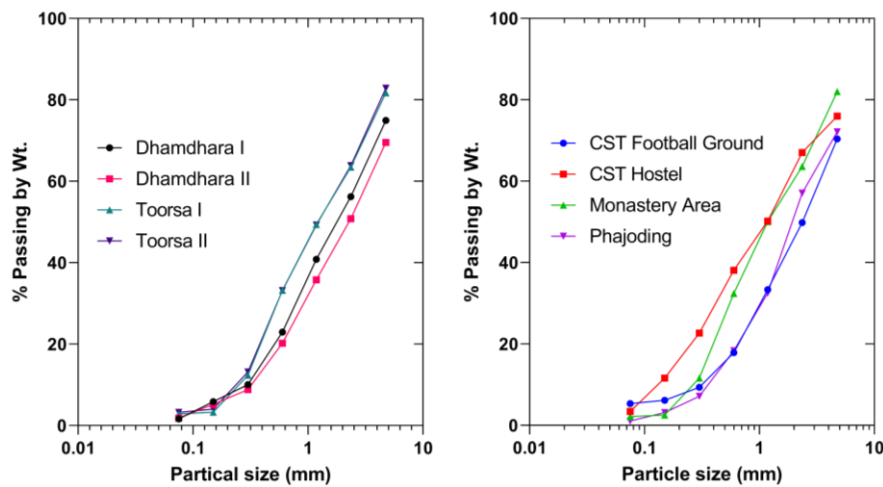
119 The geotechnical reports collected by Phuentsholing municipality have 29 stratigraphic logs. From these
120 records, the depth of the water table (GWT) was demarcated first. Drilling log data showed the highest depth of
121 the water table in the Dhamdhara area at 12.5 m to 16 m, whereas groundwater table in Rinchingding area is at 5
122 m, followed by the Torsa area at 0.5 m and 3 m, which is located near the riverbed. The depth of the water
123 table is one of the essential input parameters used for 1D ground response analysis. Three drill holes are
124 presented to typically illustrate the typical underground stratigraphy (Fig.ure 2). Table 1 presents a summary of
125 soil properties from laboratory testing of in-situ samples collected from the drill holes. The number of samples
126 in each zone represents the total number of samples collected from all drill logs at various stratigraphic depths.
127 All laboratory tests have been verified according to the Indian Standard Codes. Testing included physical
128 identification, Atterberg limits, grain size distribution and direct shear testing. Field tests such as standard
129 penetration resistance (SPT) and core cutter test were performed to determine resistance to penetration (SPT-N)
130 and field density, respectively



132 Figure 2: Typical borehole stratigraphy in Torsa and Dhamdhara (Zone I) and Rinchingding (Zone II).

133 As shown in the stratigraphic logs, the upper stratum comprises predominantly mixed coarse-grained soils
 134 characterized by dominant sand with considerable fraction of sand. The soil classification of the Phuentsholing
 135 area carried out by sieve analysis highlighted that most soils consist of 22.74% gravel, 74.89% sand, and 2.37%
 136 of the silt and clay. The sieve analysis results for the respective zones are shown in Fig. 3. The soils in Toorsa
 137 are non-plastic, as coarse-grained soils dominate the particle distribution, while the soils in Rinchending and
 138 Dhamdhara have low plasticity with a plasticity index (PI) of 6.5 and 10, respectively. The bulk density is 1.8
 139 g/cm³ in Toorsa, 1.64 g/cm³ in Dhamdhara, and 1.33 g/cm³ in Rinchending. The shear strength parameter,
 140 cohesion (c), ranges between 0-0.18 kg/cm², while the angle of internal friction (ϕ) in the study area is up to 35°.

Formatted: Indent: First line: 0"



141

142 **Figure 3:** Representative grain size distribution curve for the study area.

143 **Table 1.** Average soil parameters in the study area.

Location	Testing methods	Soil parameters	No. of samples	Reference
Toorsa (Zone I)	Atterberg's limit	Non-plastic	86	IS: 2720 (Part 5)-1995
	Core cutter	Bulk density, $\gamma_t = 1.8$ g/cc Dry density, $\gamma_d = 1.64$ g/cc		IS:2720 (Part 29)-1975
	Direct shear	$c = 0$ $\phi = 35^\circ$		IS: 2720 (Part 13)-1997
	SPT	N -value = 25 to 50		IS: 2131-1981
Dhamdhara (Zone I)	Atterberg's limit	Low plasticity (PI = 6.5)	28	IS: 2720 (Part 5)-1995
	Core cutter	Bulk density, $\gamma_t = 1.64$ g/cc Dry density, $\gamma_d = 1.51$ g/cc		IS:2720 (Part 29)-1975
	Direct shear	$c = 0.073$ kg/cm ²		IS: 2720 (Part 13)-1997

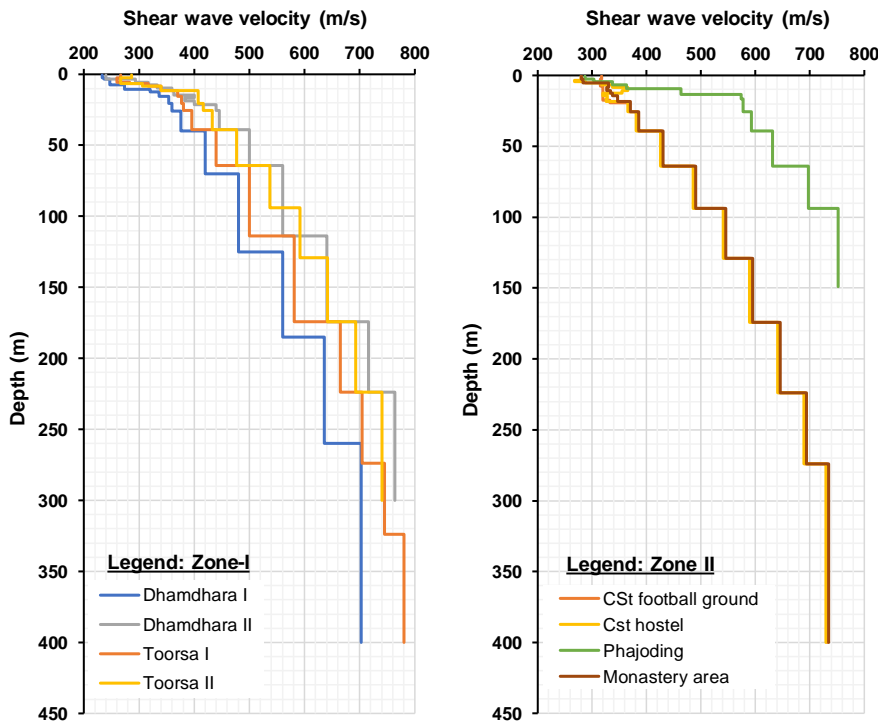
		$\phi = 31.44^\circ$		
	SPT	N -value = 19 to 37		IS: 2131–1981
Rinchending (Zone II)	Atterberg's limit	Low plasticity (PI = 10)	26	IS: 2720 (Part 5)-1995
	Core cutter	Bulk density, $\gamma_t = 1.83 \text{ g/cc}$ Dry density, $\gamma_d = 1.70 \text{ g/cc}$		IS:2720 (Part 29)-1975
	Direct shear	$c = 0.18 \text{ kg/cm}^2$ $\phi = 20-30^\circ$		IS: 2720 (Part 13)-1997
	SPT	N -value = 21 to <100		IS: 2131–1981

144

145 Shear wave velocity profiles from eight locations in the study area based on the multispectral surface
 146 wave analysis (MASW) and empirical correlation developed by (Tempa et al., 2021) are used [to perform for](#)
 147 [ground response analysis](#) [input parameters](#). According to the shear wave velocity profile, engineered bedrock (V_s
 148 > 800 m/s) lies at a depth of 150 m to 400 m as shown in Fig. 4. According to the parametric analysis carried out
 149 by (Tempa et al., 2020), the site condition in the study area is classified [into](#) as ground type B per the Euro
 150 Code EC-08 and National Earthquake Hazards Reduction Program (NEHRP) with the majority of shear velocity
 151 ($V_{s,30}$) [between values falling between](#) 380–470 m/s, except for Phajoding, which has shear wave velocity of
 152 584.76 m/s (Table 2).

153 **Table 2.** Site classification as per Euro Code EC-08

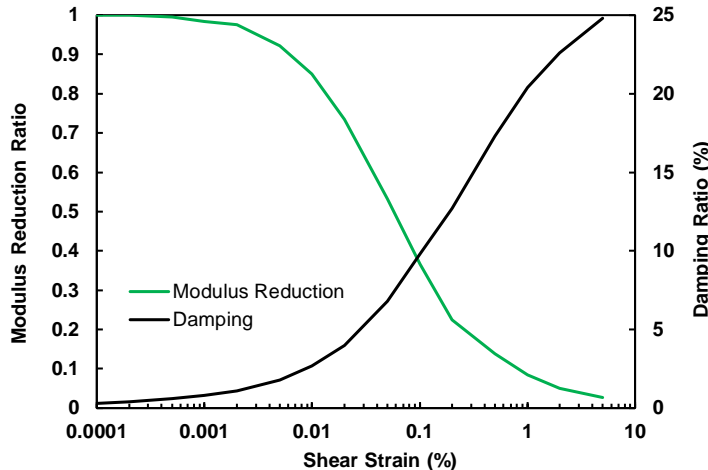
Zones	Sites	$V_{s,30}$ (m/s)	Ground Type
I	Dhamdhara I	386.43	B
	Dhamdhara II	435.92	B
	Toorsa I	439.54	B
	Toorsa II	464.30	B
II	CST football ground	426.76	B
	CST hostel	426.61	B
	Monastery area	446.20	B
All	Phajoding	584.76	B
	Bedrock	>800	A



154

155 **Figure 4:** Shear wave velocity profile of study locations in Phuentsholing, Bhutan.

156 Dynamic properties of soils are influenced by shear modulus and damping and are defined by the
 157 respective degradation models, regarded as the backbone curves. Fig. 5 represents the dynamic soil model for
 158 sand used in this study. Degradation models are well established by many investigators for different types of
 159 soils [affecting the response at low strain levels](#), (see e.g., (Seed & Idriss, 1970); (Vucetic & Dobry, 1991);
 160 (Darendeli, 2001); (Dobry & Vucetic, 1982); (Seed et al., 1986). A damped linear elastic model of the soil
 161 system is used for the analysis. Due to soil nonlinearity for which the shear modulus is strain-dependent,
 162 ProShake performs an iterative process on the linear model until both the moduli and damping ratios are
 163 compatible with the average strains and convergence is achieved at the last iteration (Shafiee et al., 2011);
 164 (Puri et al., 2018). The nonlinear and hysteretic stress-strain behavior of soils under cyclic loading is
 165 approximated as a function of G_{sec} and G_{max} . [The](#)is predetermined estimation of G_{sec} or G and G_{max} is attributed
 166 [by](#)[to](#) unit weight or bulk density, ρ , and shear wave velocity, V_s ($G_{max} = \rho V_s^2$). Similarly, damping ratios are
 167 predicted as a function of G_{sec} or G values. This estimation is achieved using an iterative procedure in the
 168 Proshake 2.0 program (EduPro Civil Systems Inc., 2017).



169

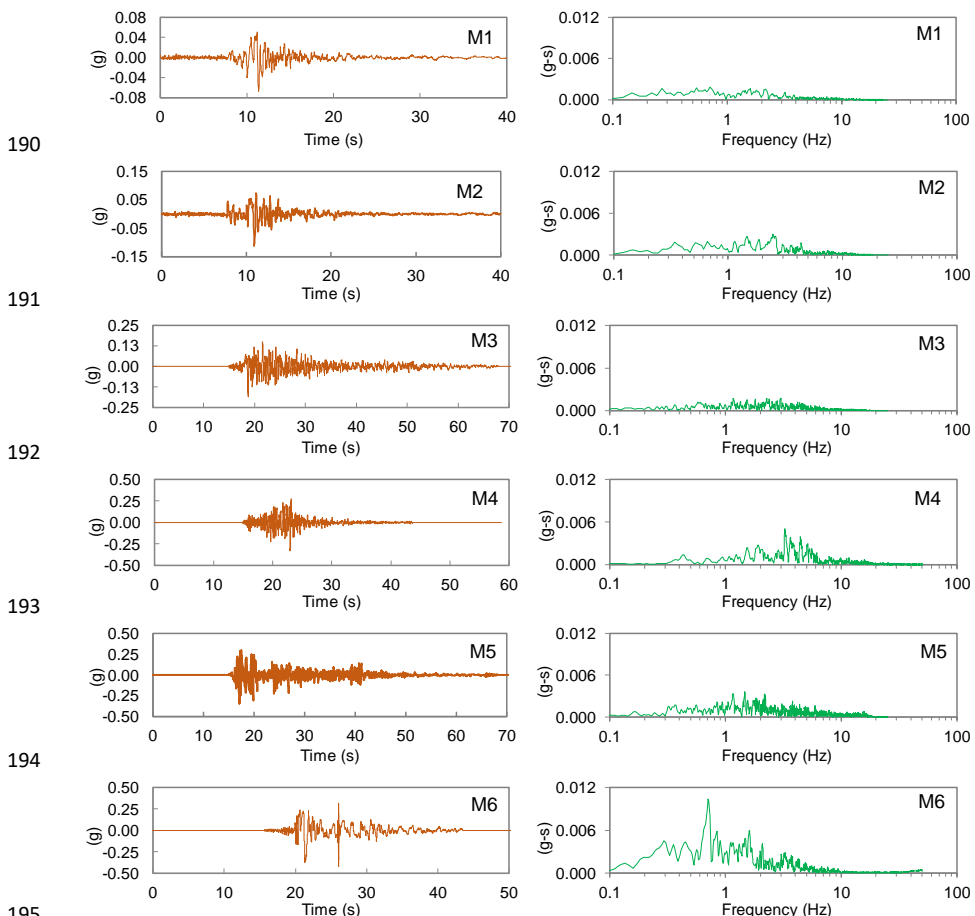
170 **Figure 5:** Average modulus reduction ratio and damping ratio adopted for sand (Seed & Idriss, 1970).171 **3.2 Selection of input motion**

172 Definition of the input motion that is considered for site response analysis of an area requires both subsurface
 173 characterization and careful selection of acceleration time histories. In Bhutan, records of acceleration time
 174 histories are very rare, if not absent. In the absence of a national seismic code, Bhutan is assumed to fall under
 175 Indian seismic zone IV and V, with an expected maximum PGA of 0.24 g and 0.36 g for design purposes. For
 176 these two zones mentioned, the PGA for earthquakes with a return period of 475 years is expected to be half of
 177 the maximum considered earthquake (MCE), i.e., 0.12 g and 0.18 g. Notably, the GSHAP depicts the PGA
 178 range between 0.2-0.28g with an increasing trend in-towards the east of the country. Considering the variations
 179 in expected PGA, we selected six acceleration time histories as input motions with PGA ranging from 0.067 g to
 180 0.422 g, considering the lowest and the highest range of possible earthquake scenarios (Table 3). The
 181 acceleration time histories used for the 1D ground response analysis are shown in Fig. 6 in ascending PGA order
 182 using the ProShake 2.0 computer program. In the ProShake 2.0 program, input motion and soil profile are
 183 denoted as “M” and “P”, respectively, and are annotated in the subsequent sections (Table 3). The amplitude
 184 and frequency content of the bedrock level motion are particularly the most important parameters (Kirtas et al.,
 185 2015); (Kramer, 1996). To understand the strong ground motion characteristics, we plotted the Fourier
 186 amplitude versus period in the frequency domain, representing the Fourier amplitude spectra of the input
 187 motions, as shown in Fig. 6. The effect of local soils is indicative at a much higher frequency range in all the
 188 investigated sites.

189 **Table 3.** Selected strong motion records for ground response analysis.

Event	Station	Year	M_w	PGA (g)	Notation
Loma Prieta/Santa Cruz Mountains	Yerba Buena Island, CA – US Coast Guard	1989	6.9	0.067	M1

Loma Prieta	Diamond Heights	1989	6.9	0.113	M2
Taft Kern County	Taft	1952	7.5	0.185	M3
Northridge	Topanga Fire Station	1994	6.7	0.329	M4
El Centro	Imperial Valley Irrigation District	1940	6.9	0.344	M5
Petrolia	Cape Mendocino	1992	6.6	0.422	M6



196 **Figure 6:** Strong motions and corresponding Fourier amplitude plots of the input ground motions.

197 **3.3 1D ground response analysis**

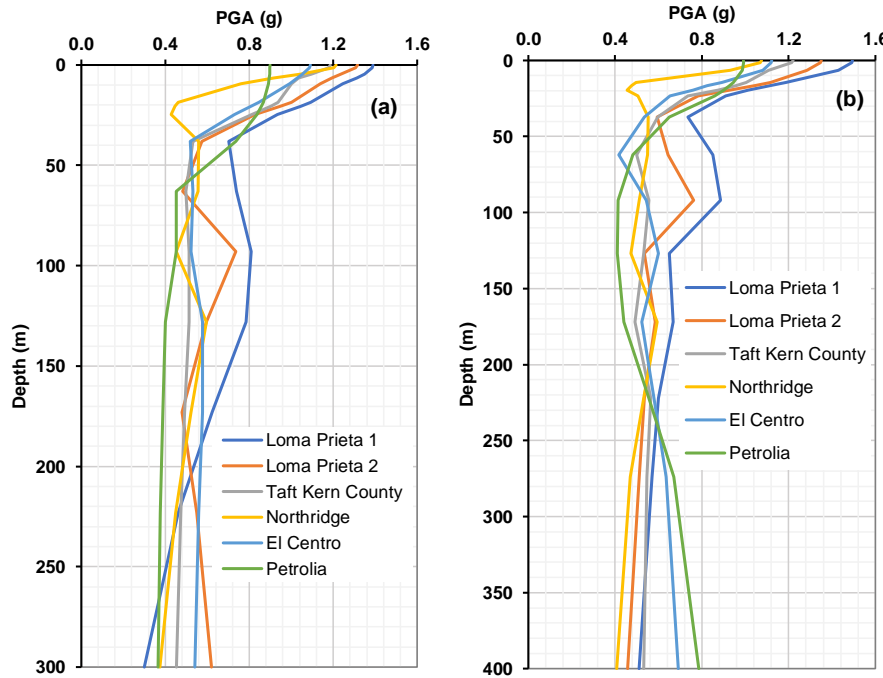
198 ~~A 1D~~ One dimensional equivalent linear analysis ~~was~~is performed at eight sites in Phuentsholing, Bhutan to
 199 estimate local site effects using the ProShake 2.0 program. In this study, six strong motion records ~~were~~are used
 200 to ~~represent~~literate low, medium, and high ~~seismic~~ acceleration categorizes ~~based on the intensity of PGA~~. The
 201 ProShake 2.0 program provides the flexibility to input ground motions and soil profiles and is useful for

202 estimating the outcrop responses to input ground shaking. The improved shear wave velocity profiles down to
203 the engineered bedrock depth (150 m and 400 m) from eight sites ~~were-are~~ used. The deep shear wave profiles
204 used in this study incorporate the effects of depth and soil type of visco-elastic soil layers above the predicted
205 engineering bedrock. The 1D ground response analysis accounts for wave propagation from the bedrock outcrop
206 through the visco-elastically stratified soil deposit and provides an estimate of the surface motion parameters.
207 The complex response method is solved by the equation of motion in the frequency domain. ~~Soil~~
208 ~~nonlinear~~~~Nonlinear~~ soil response is estimated by an iterative quasi-linear procedure in which successive linear
209 analyses are performed while updating the shear modulus and damping ratio based on the shear strain level
210 obtained from the preceding iteration. Iterations continue until the strain-compatible modulus and damping
211 converge.

212 **4. Results and discussion**

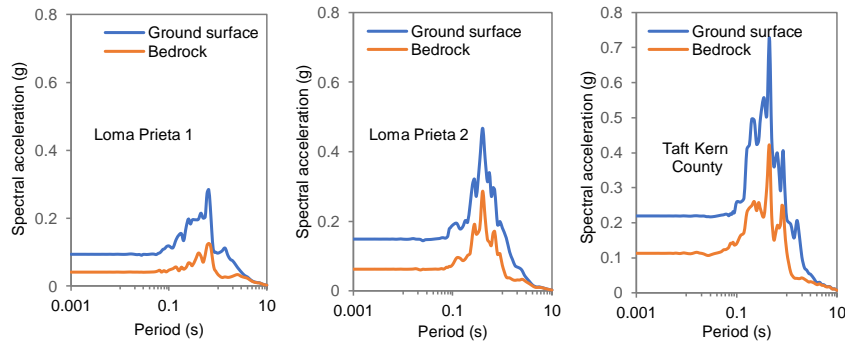
213 **4.1 Seismic site effects**

214 Fig~~ure~~ 7 shows normalized PGAs on surface at two typical locations of the investigated zones. The chart shows
215 ~~depict~~-PGA of 1.2 g to 1.5 g for low PGA earthquakes ~~and~~- 0.7 g to ~1.1 g for medium and high ~~intensity~~-PGA
216 earthquakes. Response parameters can be defined and characterized based on the amplitude parameters of the
217 ground motion and the severity of the ground motion excitation in nearby structures. This, ~~in turn~~, is a function
218 of the amplitude or intensity, the frequency content, and the duration of the ground motion (Bradley, 2011).
219 Natural periods or frequency domain parameters are related to the seismic behavior of structures and indirectly
220 reflect the ground motion characteristics (Zafarani et al., 2020). Hence, to commensurate this relationship, the
221 response spectra of bedrock and surface motion are presented in Figs. 8 and 9, ~~respectively~~. The results of
222 various input ground motions indicate ~~a-the~~ higher spectral acceleration of the soil profile in the period range
223 between 0.3 s to 3.0 s, with the peak spectral acceleration ~~range~~ of 0.14 g to 1.62 g. Thus, the structures with
224 similar fundamental vibration period~~s~~ are likely to be exposed to greater peak spectral acceleration.



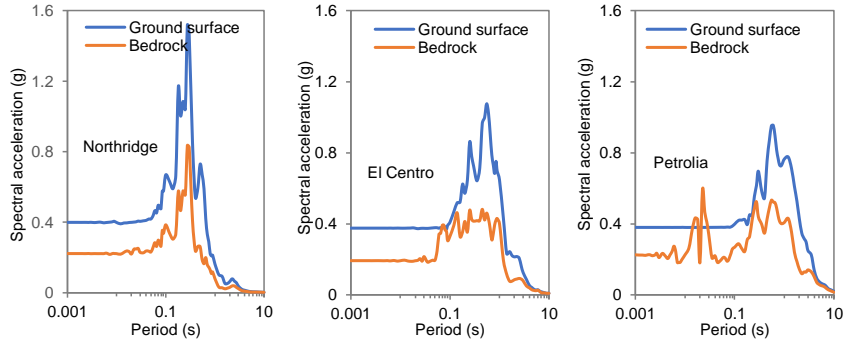
225

226 **Figure 7:** The typical profiles of normalized peak ground acceleration (PGA), (a) Toorsa II in Zone I, and (b)
227 CST Football Ground in Zone II.



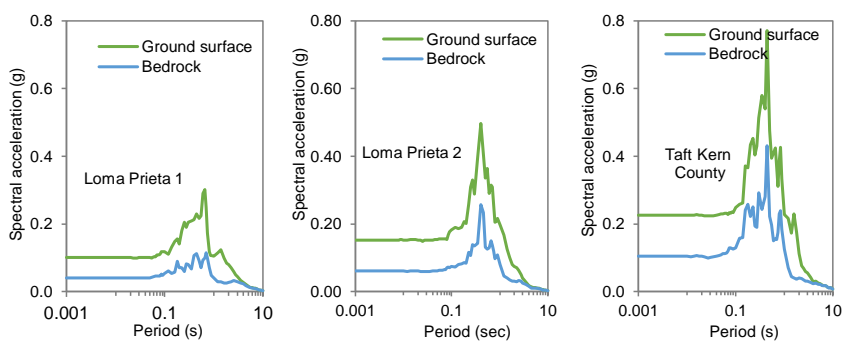
228

229



230 **Figure 8:** Typical spectral acceleration of bedrock and ground surface motion at Toorsa II in Zone I
 231 corresponding to the respective input motions.

232

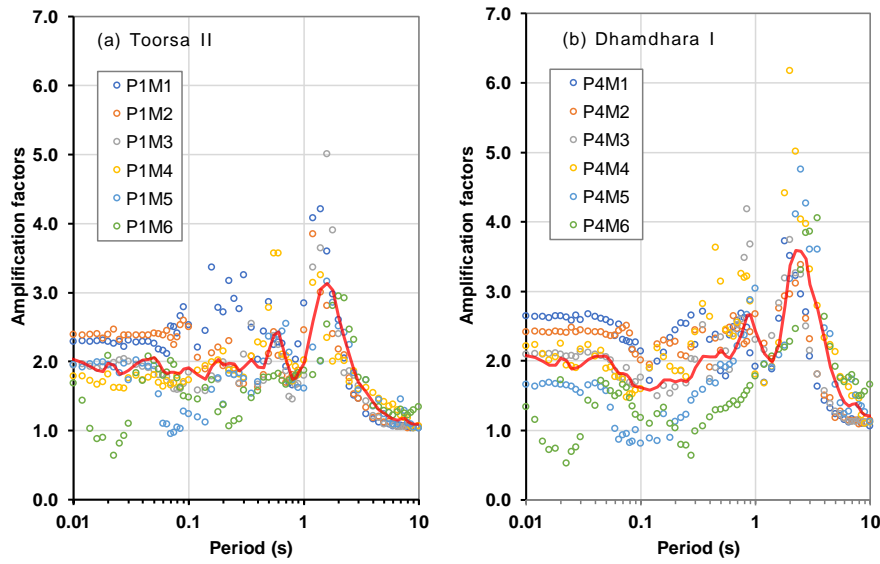


233

234 **Figure 9:** Typical spectral acceleration of bedrock and ground surface motion at CST Football Ground in Zone
 235 II corresponding to the respective input motions.

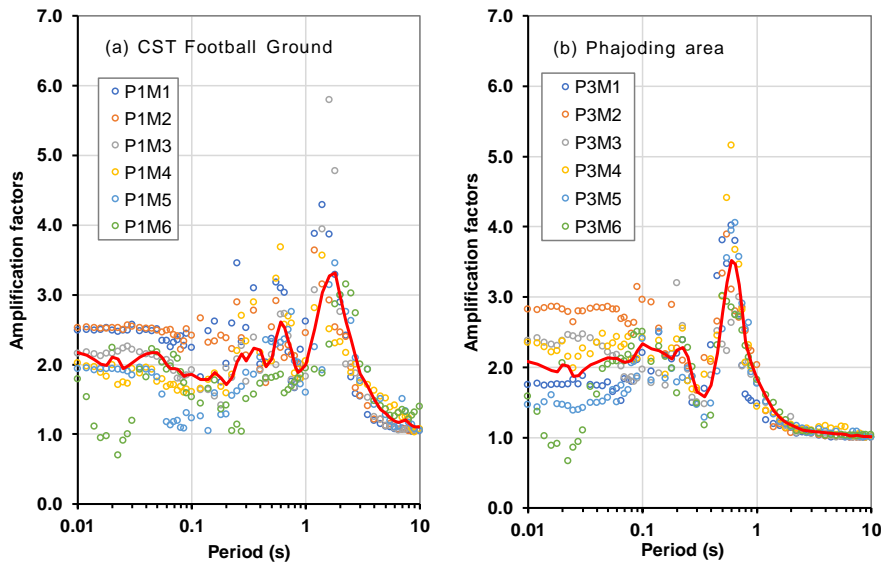
236 Figures 10 and 11 show the results of typical amplification factors at two locations in the study area.
 237 The amplification factors range from 0.7 to 2.7, 0.6 to 2.6, 0.75 to 2.5, and 0.7 to 3.2 for Toorsa II, Dhamdhara
 238 I, CST football ground, and Phajoding, respectively for 0.01 s to 0.1 s natural period. In the natural period range

239 from 0.1 to 1.0 s, the amplification factors are in the range from 1.1 to 3.6, 0.7 to 4.2, 1.0 to 3.7, and 1.2 to 5.2
 240 for Toorsa II, Dhamdhara I, CST football ground, and Phajoding, respectively. In the **high**-natural period range,
 241 the amplification factors are 5.0, 6.2, and 5.8 for Toorsa II, Dhamdhara I, and CST football ground, respectively.
 242 However, in the Phajoding the amplification factor is ~ 1.7 due to a much stiffer soil deposit ($V_{s,30} = 584.76$ m/s)
 243 and shallow engineering bedrock at 150 m.



244

245 **Figure 10:** Examples of amplification factors for various earthquakes at (a) Soil profile P1 at Toorsa II in Zone
 246 I, (b) Soil profile P4 at Dhamdhara I in Zone I.



247

248 **Figure 11:** Examples of amplification factors for various earthquakes at (a) Soil profile P1 at CST Football
 249 Ground in Zone II, (b) Soil profile P3 at Phajoding in Zone II.

250 **4.2 Correlation analysis**

251 The main objective of this study is to demonstrate the sensitivity of input motion amplitudes to predict the
 252 variability of seismic site effects due to local ground conditions. We ~~aim to examine~~ examined the potential
 253 trends, patterns, and relationships between data sets for the numerical results, obtained from the analysis. Using
 254 statistical analysis, variation of amplitude parameters is projected by box plots (Figs. 12 and 13). Statistical
 255 correlations are fitted between peak ground acceleration (PGA), peak ground velocity (PGV), peak ground
 256 displacement (PGD), and spectral acceleration (S_a) to determine the correlation between the effects of strong
 257 ground motion and the local soil conditions. As anticipated, the 1992 Petrolia earthquake with 0.422 g PGA
 258 ($M_w = 6.6$) led to the greatest response. However, the 1994 Northridge earthquake with a PGA of 0.329 g (M_w
 259 = 6.7) shows greater variability in spectral acceleration compared to other earthquakes. This is because the
 260 spectral acceleration ~~is one of the most important response parameters~~ corresponds to the interaction between
 261 the ground and the shaking intensity of an earthquake, ~~and is directly related to the response of equivalent SDOF~~
 262 ~~systems~~. Therefore, from the perspectives of seismic site effects the box plot of the spectral acceleration (period
 263 or frequency domain) is highly scattered with the outliers, confirming uncertainty in the ground response
 264 characteristics in both regions. The El Centro and Petrolia earthquakes, with the highest PGAs, also appear to be
 265 closely associated with spectral acceleration.

266

267

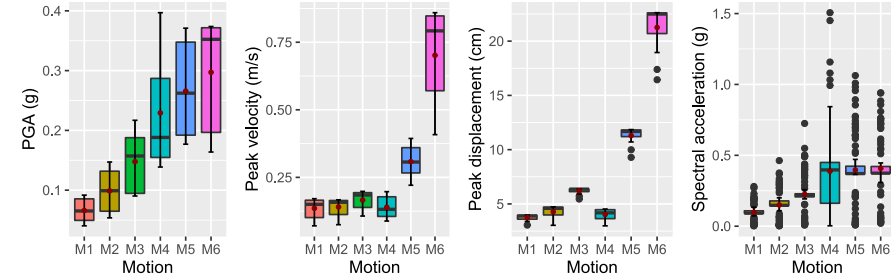


Figure 12: Box and Whisker plot for ground motion parameters of soil profile at P1 Toorsa II in Zone I.

268

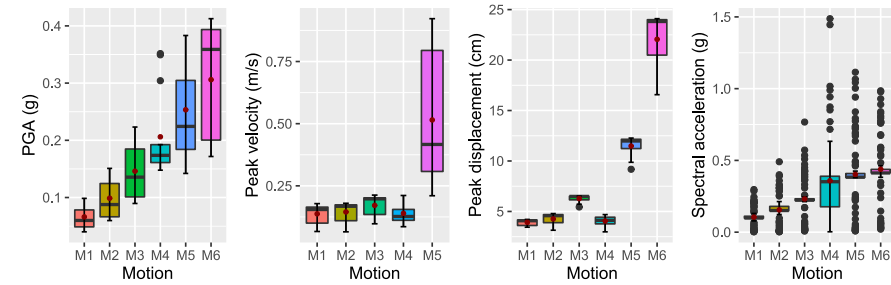
269
270

Figure 13: Box and Whisker plot for ground motion parameters of the soil profile at P1 CST Football Ground in Zone II.

Formatted: Left

271

272

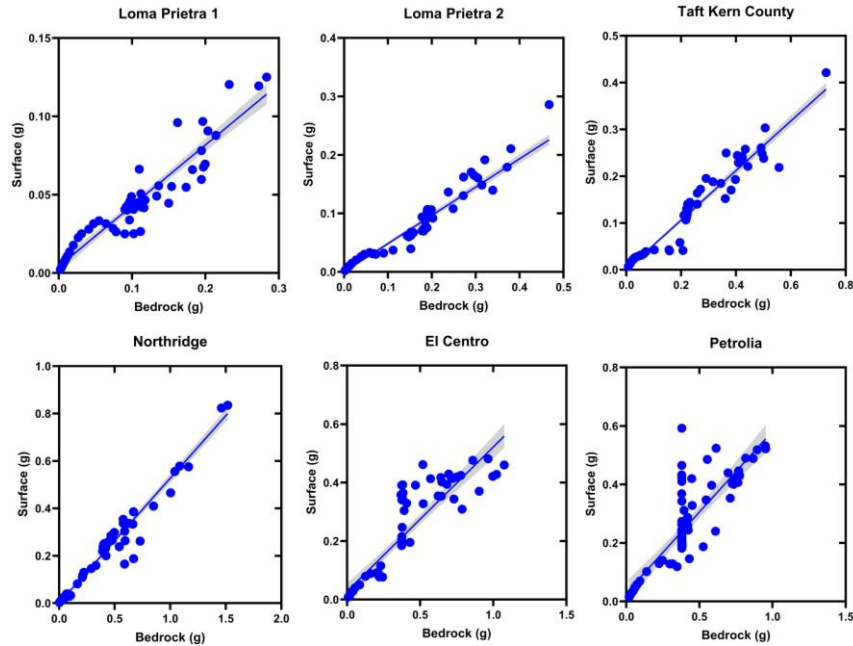
273

274

275

276

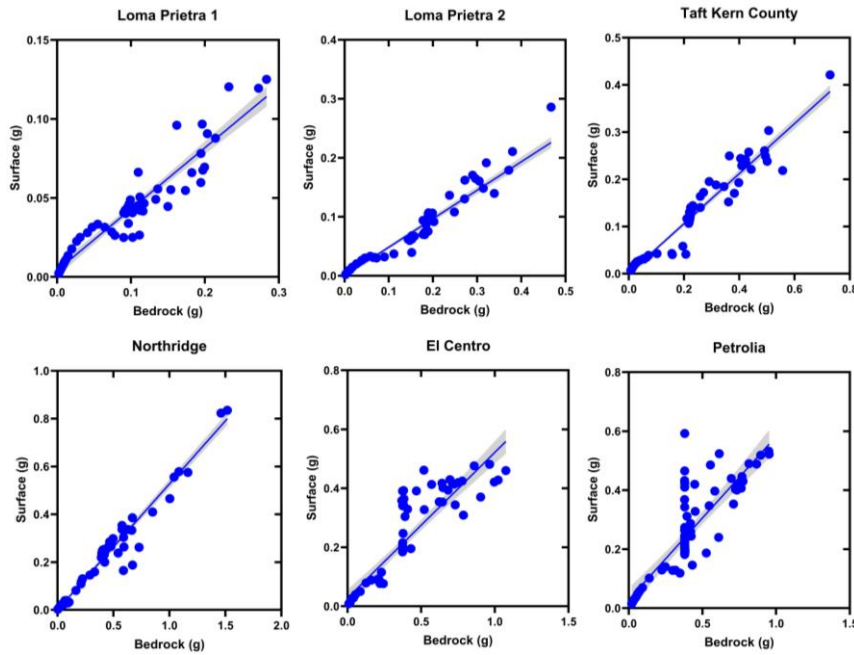
Primarily, propagating energy waves (outcrop motion) act on each stratified soil layers that amplifies or de-amplifies the ground motion response parameters at each layer. The sensitivity of the input motion parameters is critically monitored, and enhanced correlations are developed. To outline this, a linear regression model for bedrock outcrop motion and the predicted motion parameters as a function of bedding depth is developed. Regression analysis is performed for one particular soil profile from two zones (Toorsa II and CST Hostel) in order to accurately substantiate sensitivity analysis (Figs. 14 and 15).



277

278 **Figure 14:** Linear regression model for bedrock and surface spectral accelerations for Toorsa II (Zone I).

279 The 95% confidence interval (CI) shows a linear relationship for the Loma Prieta 2, Taft Kern County, and
 280 Northridge earthquakes indicate a closer impact on surface motion that corresponds *the* outcrop motion. In this
 281 case, the predominant frequency content of the input motion is between 1 and 10 Hz. In contrast, the Loma
 282 Prieta 1, El Centro, and Petrolia earthquakes, with a predominant frequency between 0.3 and 1.2 Hz, exhibit
 283 typical nonlinearity throughout the spectral range, indicating possible damping of the spectral responses of the
 284 soil deposits.



285

286 **Figure 15:** Linear regression model for bedrock and surface spectral accelerations for CST Hostel (Zone II)
 287 Sensitivity of input motion.

288 Since all analysis sites are in type B site, the trend of ground motion variation to surface is very similar, so the
 289 average values may be crucial for better implementation of the scenario-based seismic risk in the study area.
 290 Ground response parameters such as [the PGA](#) and response spectrum intensity including [the Arias](#) intensity
 291 show linear variation for aggregated values while increasing intensity of earthquake shaking corresponding to a
 292 given soil profile. The mean, median, and standard deviation of the output parameters are computed. The
 293 response spectrum intensity is computed based on Housner approach (Housner, 1959) as integral from 0.1 to 2.5
 294 s of the pseudo-velocity spectrum that provides an indication of the average velocity for most civil engineering
 295 structures. The plot of sensitivity of various input motions on amplitude parameters to different local soils [in-for](#)
 296 [the two study](#) zones is shown in Figs. 16 and 17.

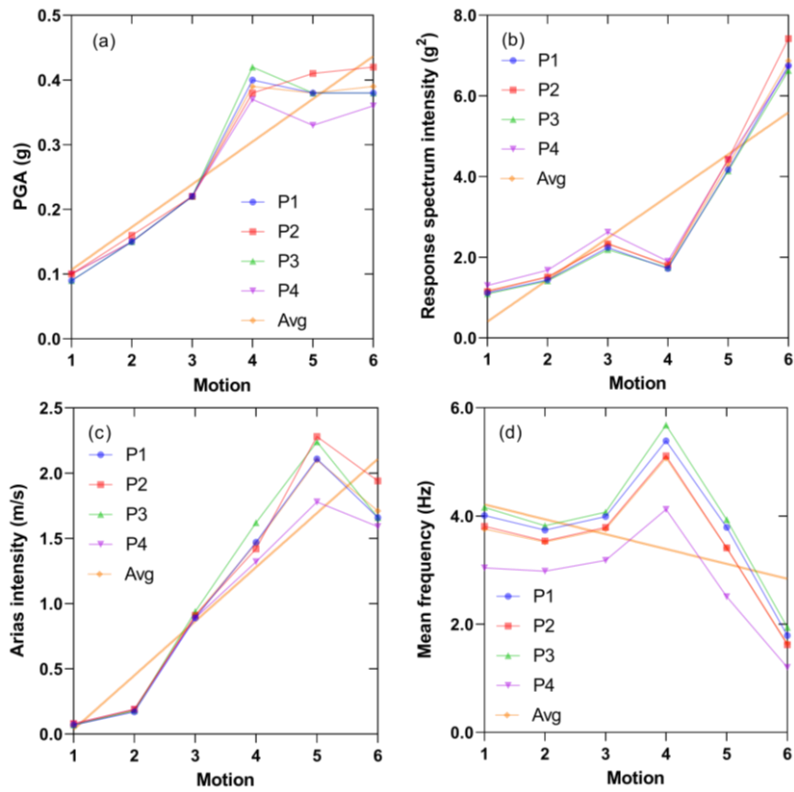
297 The standard deviation is lower for a set of predominant natural periods for a soil profile compared to
 298 the response spectrum dataset and [the](#) deviation from the mean value indicates [a](#) stronger soil response to the
 299 SDOF systems, as shown in Table 4 and Table 5. Soil nonlinearity often shows a significant scatter in spectral
 300 acceleration at higher and lower periods, and therefore the practical reliability of the result is that it prompts
 301 more analysis [with many](#)[with many](#) input motions to predict the mean (or median) response with some level of
 302 confidence (Kramer et al., 2012).[\(Kramer et al., 2012\)](#) The sensitivity of input motion is shown in Figs. 14
 303 and 15 from two investigated locations. The results of the correlation analysis and the sensitivity plots indicate
 304 that the input motion M4 (Northridge) has a significant influence on most of the response parameters. The
 305 additional ground response parameters are provided in [the appendix](#) (Tables SA1 and Table SA2).

306 **Table 4.** Descriptive statistics for averaged ground response parameters in Zone I for all four soil profiles and
 307 six input ground motions.

	PGA (g)	Aries intensity (m/sec)	Response spectrum intensity (g ²)	Predominant period (sec)	Mean frequency (Hz)
Mean	0.270	1.073	2.996	0.818	3.527
Median	0.238	0.630	2.450	0.689	3.319
Standard deviation	0.121	0.765	2.013	0.468	1.097
84 th percentile	0.407	2.215	4.541	1.251	4.824
16 th percentile	0.139	0.179	1.322	0.379	2.283

308 **Table 5.** Descriptive statistics for averaged ground motion parameters in Zone II for all four soil profiles and six
 309 input ground motions.

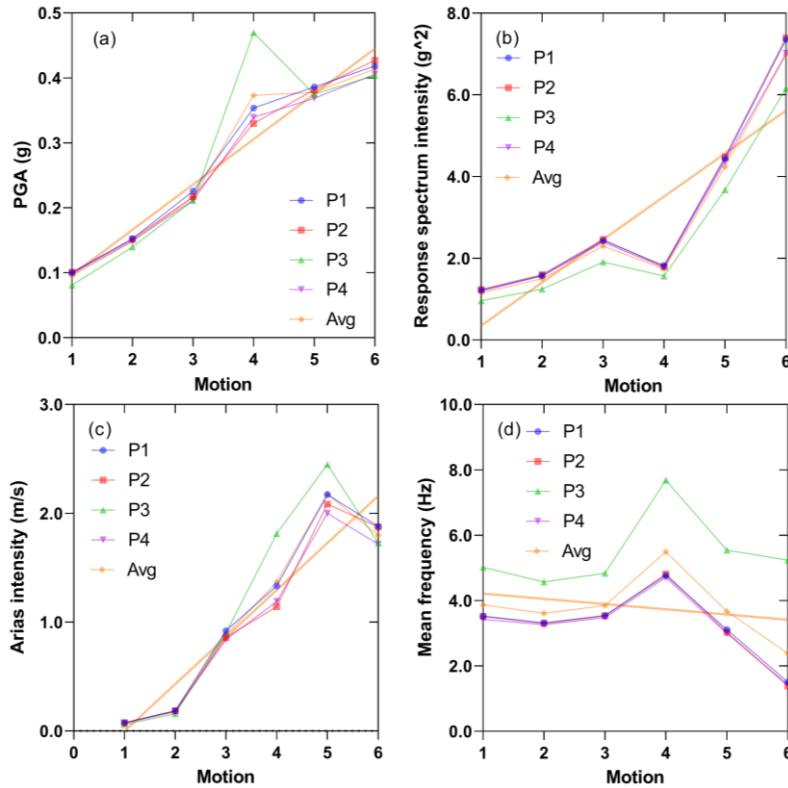
	PGA (g)	Arias intensity (m/s)	Response spectrum intensity (g ²)	Predominant period (s)	Mean frequency (Hz)
Mean	0.271	1.079	2.985	0.812	3.814
Median	0.237	0.622	2.417	0.684	3.538
Standard deviation	0.126	0.794	2.066	0.453	1.382
84 th percentile	0.411	2.226	4.541	1.243	5.330
16 th percentile	0.136	0.174	1.287	0.377	2.349



310

311 **Figure 16:** Sensitivity of input ground motion in Zone I. (a) Peak ground acceleration,
 312 (b) Response spectrum intensity,
 313 (c) Arias intensity, (d) Mean frequency. Soil profiles P1: Toorsa II, P2: Toorsa 1, P3: Dhamdhara II
 and P4: Dhamdhara I.

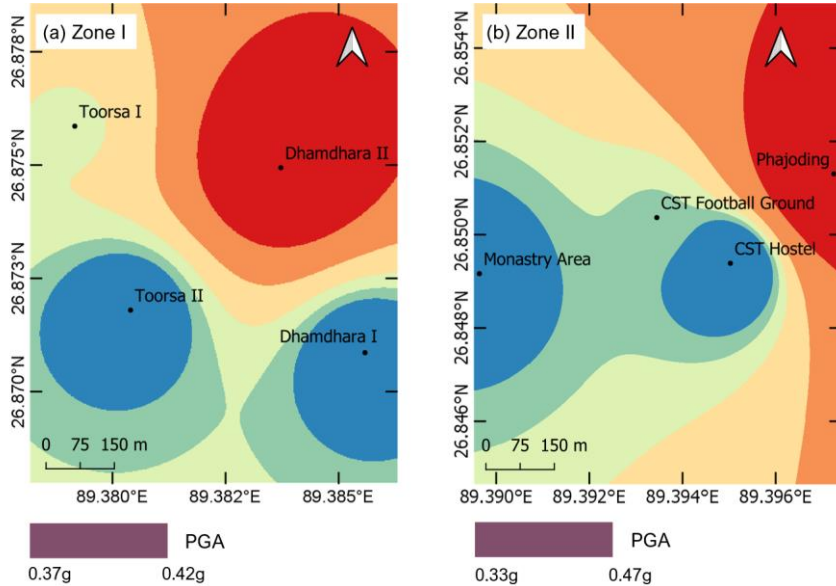
314



315

316 **Figure 17:** Sensitivity of input ground motion in Zone II. (a) Peak ground acceleration
 317 (b) Response spectrum intensity, (c) Arias intensity, (d) Mean frequency. Soil profiles P1: CST Football Ground, P2: CST Hostel, P3:
 318 Phajoding, and P4: Monastery area

319 In this study, the The PGA of M4 (Northridge) are mapped to show the spatial variability in two zones
 320 as shown in Fig. 18. The PGA in Zone I are-is distributed between 0.37 g to 0.42 g. The variability of PGA in
 321 Zone II is higher compared to Zone I as, resulting in the PGA range for Zone II is 0.33 g to 0.47 g. The resulting
 322 interplay of strong ground motion parameters with local soil conditions primarily highlights the importance of
 323 the current study on the significance of input motion characterization.



324

325 **Figure 18:** PGA distribution map of input motion M4 Northridge earthquake, (a) Toorsa and Dhamdhara in
 326 Zone I, (b) Rinchending in Zone II.

327 **5. Conclusions**

328 Using 1D site response analysis, we performed sensitivity of various input motions. [Ground motion parameter](#)
 329 [sensitivity for soft soil deposits is assessed considering typical eastern Himalayan setting. Aiming to quantify](#)
 330 [the variation of input motion characteristics, we assessed several ground motion parameters. The conclusions of](#)
 331 [the study can be depicted as follows: The study concludes the following:](#)

- 332 • The trend in the variation of ground motion parameters such as PGA, PGD, PGV, and SA projects an
 333 increasing order with ground motion intensity as expected. [However, the ground motions with input PGA](#)
 334 [greater than 0.34g and less than 0.1g are more sensitive than the others. This concludes that sensitivity is](#)
 335 [more prominent in low and high PGA range than the moderate shaking scenario \(0.1-0.34g\).](#)
- 336 • [The correlation analysis and linear regression models provide the enhanced characteristics of input](#)
 337 [motion propagation, indicating possible use of earthquake PGA between 0.11 g and 0.33 g from 1 to 10 Hz](#)
 338 [frequency.](#)
- 339 • For loose soil sites characterized as type B ground, peak spectral acceleration is prominent between 0.3 to 3
 340 sec, this implies that the structures with their fundamental vibration period between 0.3 to 3 sec will
 341 observe greater peak spectral acceleration. Consideration of earthquake resistant design for the structures
 342 with fundamental vibration period requires additional attention due to the severity in peak spectral
 343 acceleration occurrence.
- 344 • In general, the peak amplification factor is obtained up to 6.2 for the study area. The lower amplification
 345 factor coincides the occurrence of bedrock early. Meanwhile, the soil columns with greater depth of loose

Formatted: Font: (Default) Times New Roman, 10 pt
 Complex Script Font: Times New Roman, 10 pt

Formatted: Indent: Left: 0.25", No bullets or numbering

346 soil deposits have reflected greater amplification. The spatial variation of amplification factor is quite
347 significant even in a small area. Thus, more rigor is necessitated for site response analysis and
348 microzonation studies in soft soil deposits to incorporate the spatial variation in soil columns. If soil
349 stiffness is increased, the amplification factor can be checked, thus, soil improvement may be required to
350 assure foundation performance in loose soil deposit.

351 This study uses various strong motions to depict the variability ground motion characteristics. Although this is
352 one of the first studies in the area, the results are still preliminary and detailed investigation using sophisticated
353 soil characteristics and approaches could effectively in obtaining more reliable results.

- 354 • The surface PGA in the investigation area of site classification type B shows 0.1 g to 0.15 g for the
355 earthquake of low intensity, 0.23 g to ~ 0.38 g for the earthquake of medium intensity, and more than 0.43 g
356 for an earthquake of high PGA earthquakes. The result shows a higher spectral acceleration in a period
357 range from 0.3 s to 3.0 sec with approximately 0.14 g to 1.62 g peak spectral acceleration.
- 358 • The critical range of the fundamental natural period is roughly between 0.9 sec to ~ 5.0 sec with the highest
359 range of seismic wave amplification being between ~ 2.8 to 6.2. In Phajoding, the significance of
360 amplification is comparatively less at ~ 1.7 between 0.4 s and 1.0 s due to a much stiffer soil deposit ($V_{s,30} =$
361 584.76 m/s) and a shallow engineering bedrock at 150 m.
- 362 • This study indicated some anomalies in seismic site effects due to input motion. Therefore, an appropriate
363 ground motion characterization is recommended for site specific seismic analysis. The high Fourier
364 amplitude characteristics at low frequency have a greater tendency to reflect anomalies in response
365 parameters.

366 Data availability

367 All the data used in this study are presented in the paper.

368 Author contribution

369 Conceptualization (KT), Data curation (KT), Formal analysis (KT), Funding acquisition (KRA), Methodology
370 (KT, DG and GF), Resources (KT, DG and KRA), Software and visualization (KT), Writing – original draft
371 preparation (KT), Writing – review & editing (DG, NC, GF and KRA).

372 Competing interests

373 The authors declare that they have no competing interests.

374 Acknowledgements

375 The authors are thankful to Phuentsholing Thromde (Municipal office) for providing additional geotechnical
376 data.

Formatted: Normal, No bullets or numbering

Formatted: Font: (Default) Times New Roman, 10 pt
Complex Script Font: Times New Roman, 10 pt

377 **References**

378 Berthet, T., Hetényi, G., Cattin, R., Sapkota, S. N., Champollion, C., Kandel, T., Doerflinger, E., Drukpa, D.,
379 Lechmann, S., and Bonnin, M.: Lateral uniformity of India Plate strength over central and eastern Nepal,
380 Geophysical Journal International, 195(3), 1481–1493, <https://doi.org/10.1093/gji/ggt357>, 2013.

381 Bhutani, M., and Naval, S.: Preliminary amplification studies of some sites using different earthquake motions,
382 Civil Engineering Journal (Iran), 6(10), 1906–1921, <https://doi.org/10.28991/cej-2020-03091591>, 2020.

383 Bommer, J. J., and Martinez-Pereira, A.: Strong-motion parameters: definition, usefulness and predictability,
384 12th World Conference on Earthquake Engineering, 1–8, <http://www.iitk.ac.in/nicee/wcee/article/0206.pdf>,
385 2000.

386 Bradley, B. A.: Empirical correlation of PGA, spectral acceleration and spectrum intensities from active shallow
387 crustal earthquakes, Earthquake Engineering and Structural Dynamics, 40(15), 1–15.
388 <https://doi.org/10.1002/eqe>, 2011.

389 Chavez-Garcia, F. J., Pedotti, G., Hatzfeld, D., and Bard, P. Y.: An experimental study of site effects near
390 Thessaloniki (northern Greece), Bulletin - Seismological Society of America, 80(4), 784–806, 1990.

391 Chettri, N., Gautam, D., and Rupakhetty, R.: From Tship Chim to Pa Chim: Seismic vulnerability and
392 strengthening of Bhutanese vernacular buildings, In R. Rupakhetty and D. Gautam (Ed.), Masonry Construction
393 in Active Seismic Regions (1st ed. Ca, Issue May, pp. 253–288), Elsevier, <https://doi.org/10.1016/c2019-0-02453-3>, 2021. a

395 Chettri, N., Gautam, D., and Rupakhetty, R.: Seismic vulnerability of vernacular residential buildings in Bhutan,
396 Journal of Earthquake Engineering, 26(1), 1–16. <https://doi.org/10.1080/13632469.2020.1868362>, 2021. b

397 Darendeli, M. B.: Development of a New Family of Normalized Modulus Reduction and Material Damping
398 Curves, Dept. of Civil Eng., Univ. of Texas, Austin, 2001

399 Dobry, R., and Vucetic, M.: Dynamic properties and seismic response of soft clay deposits, International
400 Symposium on Geotech., Eng. of Soft Soils, Maxico, 2(January 1987), 51–87, 1982.

401 Douglas, J.: Selection of strong-motion records for use as input to the structural models of VEDA, BRGM,
402 2006.

403 Drukpa, D., Velasco, A. A., and Doser, D. I.: Seismicity in the Kingdom of Bhutan (1937-2003): Evidence for
404 crustal transcurrent deformation, Journal of Geophysical Research: Solid Earth, 111(6), 1–14,
405 <https://doi.org/10.1029/2004JB003087>, 2006.

406 EduPro Civil Systems Inc.: ProShake: Ground Response Analysis Program 2.0, User's Manual. 2017.

407 Gautam, D.: Mapping surface motion parameters and liquefaction susceptibility in Tribhuvan International
408 Airport, Nepal, Geomatics, Natural Hazards and Risk, 8(2), 1173–1184,
409 <https://doi.org/10.1080/19475705.2017.1305993>, 2017.

410 Gautam, D., and Chamlagain, D.: Preliminary assessment of seismic site effects in the fluvio-lacustrine
411 sediments of Kathmandu valley, Nepal, *Natural Hazards*, 81(3), 1745–1769, <https://doi.org/10.1007/s11069-016-2154-y>, 2016.

413 Gautam, D., Forte, G., and Rodrigues, H.: Site effects and associated structural damage analysis in Kathmandu
414 Valley, Nepal. *Earthquake and Structures*, 10(5), 1013–1032, <https://doi.org/10.12989/eas.2016.10.5.1013>,
415 2016.

416 Housner, G.W.: Behavior of structures during earthquakes, *Journal of the Engineering Mechanics Division*,
417 ASCE, 85(14), 109–129, 1959.

418 ISSMGE.: Manual for zonation on seismic geotechnical hazards. In: Technical committee for earthquake
419 geotechnical engineering, TC4, international society for soil mechanics and geotechnical engineering, The
420 Japanese Geotechnical Society, Tokyo, 1999.

421 IS:1893.: Criteria for Earthquake Resistant Design of Structures - General Provisions and Buildings Part-1,
422 Bureau of Indian Standards, New Delhi, Part 1, 1–39, 2002.

423 Jishnu, R. B., Naik, S. P., Patra, N. R., and Malik, J. N.: Ground response analysis of Kanpur soil along Indo-
424 Gangetic Plains, *Soil Dynamics and Earthquake Engineering*, 51(2013), 47–57,
425 <https://doi.org/10.1016/j.soildyn.2013.04.001>, 2013.

426 Kirtas, E., Koliopoulos, P., Kappos, A., Theodoulidis, N., Savvaidis, A., Margaris, B., and Rovithis, E.:
427 Identification of earthquake ground motion using site effects analysis in the case of Serres city, Greece,
428 *International Journal of Civil Engineering and Architecture*, 2(1), 20–27, 2015.

429 Kramer, S. L.: *Geotechnical Earthquake Engineering*, Prentice Hall, 1996.

430 Kramer, S. L., Arduino, P., and Sideras, S. S.: Earthquake ground motion selection, The State of Washington
431 Department of Transportation, 2012.

432 Long, S., and McQuarrie, N.: Placing limits on channel flow: Insights from the Bhutan Himalaya, *Earth and
433 Planetary Science Letters*, 290(3–4), 375–390, <https://doi.org/10.1016/j.epsl.2009.12.033>; 2010.

434 Lopez-Caballero, F., Gelis, C., Regnier, J., and Bonilla, L. F.: Site response analysis including earthquake input
435 ground motion and soil dynamic properties variability, 15th World Conference on Earthquake Engineering,
436 2012.

437 Licata, V., Forte, G., d'Onofrio, A., Santo, A., Silvestri, F.: A multi-level study for the seismic microzonation of
438 the Western area of Naples (Italy), *Bulletin of Earthquake Engineering*, 17(9), 4711–4741, 2019.

439 McQuarrie, N., Long, S. P., Tobgay, T., Nesbit, J. N., Gehrels, G., and Ducea, M. N.: Documenting basin scale,
440 geometry and provenance through detrital geochemical data: Lessons from the Neoproterozoic to Ordovician
441 Lesser, Greater, and Tethyan Himalayan strata of Bhutan, *Gondwana Research*, 23(4), 1491–1510,
442 <https://doi.org/10.1016/j.gr.2012.09.002>, 2013.

443 Naik, S. P., and Patra, N. R.: Generation of Liquefaction Potential Map for Kanpur City and Allahabad City of
444 Northern India: An Attempt for Liquefaction Hazard Assessment, Geotechnical and Geological Engineering,
445 36(1), 293–305, <https://doi.org/10.1007/s10706-017-0327-4>, 2018.

446 Nath, S. K., and Thingbaijam, K. K. S.: Seismic hazard assessment - A holistic microzonation approach, Natural
447 Hazards and Earth System Science, 9(4), 1445–1459, <https://doi.org/10.5194/nhess-9-1445-2009>, 2009.

448 Panjamani, A., Katukuri, A. K., Reddy, G. R., Moustafa, S. S. R., and Al-Arifi, N. S. N.: Seismic site
449 classification and amplification of shallow bedrock sites, PLoS ONE, 13(12), 1–22,
450 <https://doi.org/10.1371/journal.pone.0208226>, 2018.

451 Puri, N., Jain, A., Mohanty, P., and Bhattacharya, S.: Earthquake Response Analysis of Sites in State of Haryana
452 using DEEPSOIL Software, Procedia Computer Science, 125(January), 357–366,
453 <https://doi.org/10.1016/j.procs.2017.12.047>, 2018.

454 Seed, H. B., and Idriss, I. M.: Soil Moduli and Damping Factors for Dynamic Response Analyses [Report No.
455 EERC 70-10], Earthquake Engineering Research Centre, University of California, Berkeley,
456 <https://ntrl.ntis.gov/NTRL/dashboard/searchResults/titleDetail/PB197869.xhtml>, 1970.

457 Seed, H. B., Wong, R. T., Idriss, I. M., and Tokimatsu, K.: Moduli and Damping Factors for Dynamic Analyses
458 of Cohesionless Soils, Journal of Geotechnical Engineering, 112(11), 1016–1032, 1986.

459 Shafiee, A., Kamalian, M., Jafari, M. K., and Hamzehloo, H.: Ground motion studies for microzonation in Iran,
460 Natural Hazards, 59(1), 481–505, <https://doi.org/10.1007/s11069-011-9772-1>, 2011.

461 Shiuly, A., and Narayan, J. P.: Deterministic seismic microzonation of Kolkata city. Natural Hazards, 60(2),
462 223–240, <https://doi.org/10.1007/s11069-011-0004-5>, 2012.

463 Sil, A., and Haloi, J.: Site-specific ground response analysis of a proposed bridge site over Barak River along
464 Silchar Bypass Road, India, Innovative Infrastructure Solutions, 3(1), <https://doi.org/10.1007/s41062-018-0167-y>, 2018.

466 Sitharam, T. G.: Seismic Microzonation: Principles, Practices and Experiments, Electronic Journal of
467 Geotechnical Engineering, 1–58, 2008.

468 Sitharam, T. G., Anbazhagan, P., Mahesh, G. U., Bharathi, K., and Reddy, P. N.: Seismic Hazard Studies Using
469 Geotechnical Borehole Data and GIS, Symposium on Seismic Hazard Analysis and Microzonation, 341–358,
470 2005.

471 Stevens, V. L., De Risi, R., Le Roux-Mallouf, R., Drukpa, D., and Hetényi, G.: Seismic hazard and risk in
472 Bhutan, Natural Hazards, 104(3), 2339–2367, <https://doi.org/10.1007/s11069-020-04275-3>, 2020.

473 Tempa, K., and Chettri, N.: Comprehension of Conventional Methods for Ultimate Bearing Capacity of Shallow
474 Foundation by PLT and SPT in Southern Bhutan, Civil Engineering and Architecture, 9, 375–385,
475 <https://doi.org/10.13189/cea.2021.090210>, 2021.

476 Tempa, K., Chettri, N., Gurung, L., and Gautam, D.: Shear wave velocity profiling and ground response analysis
477 in Phuentsholing, Bhutan, Innovative Infrastructure Solutions, 6(2), 1–16, <https://doi.org/10.1007/s41062-020-00420-w>, 2021.

479 Tempa, K., Chettri, N., Sarkar, R., Saha, S., Gurung, L., Dendup, T., and Nirola, B. S.: Geotechnical parameter
480 assessment of sediment deposit: A case study in Pasakha, Bhutan, Cogent Engineering, 8(1), 1–21,
481 <https://doi.org/10.1080/23311916.2020.1869366>, 2021.

482 Tempa, K., Sarkar, R., Dikshit, A., Pradhan, B., Simonelli, A. L., Acharya, S., and Alamri, A. M.: Parametric
483 study of local site response for bedrock ground motion to earthquake in Phuentsholing, Bhutan, Sustainability
484 (Switzerland), 12(13), 1–20, <https://doi.org/10.3390/su12135273>, 2020.

485 Vucetic, M., and Dobry, R.: Effect of Soil Plasticity on Cyclic Response. Journal of Geotechnical Engineering,
486 117(1), 89–107, <http://sokocalo.enr.ucdavis.edu/~jeremic/PAPERSlocalREPO/CM1769.pdf>, 1991.

487 Wyss, M., and Rosset, P.: Mapping seismic risk: The current crisis. Natural Hazards, 68(1), 49–52,
488 <https://doi.org/10.1007/s11069-012-0256-8>, 2013.

489 Zafarani, H., Ghafoori, S. M. M., Soghrat, M. R., and Shafiee, M.: Spatial correlation of peak ground motions
490 and pseudo-spectral acceleration based on the sarpol-e-zahab mw 7.3, 2017 earthquake data, Annals of
491 Geophysics, 63(4), 1–15, <https://doi.org/10.4401/ag-8349>, 2020.